

Chapter 20

Optimal Microgrid Operational Planning Considering Distributed Energy Resources



Mehrdad Setayesh Nazar, Ainollah Rahimi Sadegh and Alireza Heidari

Abstract This chapter introduces an approach for Optimal Microgrid Operational Planning (OMOP) considering wind and photovoltaic power generations, combined heat and power generation units, electrical energy storages and interruptible loads. The problem explores the optimal maintenance scheduling and operational planning of a microgrid. A framework for OMOP is presented based on a two-level optimization procedure taking into account the system uncertainties. The formulated problem is modelled as a Mixed Integer Nonlinear Programming (MINLP) problem and a heuristic optimization method is utilized for the first level problem; meanwhile, a MINLP solver is used for the second level problem. This model is applied to the 9-bus and 33-bus test systems and the numerical results assess the effectiveness of the introduced method.

Keywords Microgrid · Maintenance scheduling · Optimal operational planning · Heuristic optimization

Nomenclature

C_{MC}	Maintenance cost
C_{OP}	Operation cost
X	Decision variable of maintenance
N_{sub}	Number of substations

M. Setayesh Nazar (✉) · A. Rahimi Sadegh
Faculty of Electrical Engineering, Shahid Beheshti University, A.C., Tehran, Iran
e-mail: m_setayesh@sbu.ac.ir

A. Rahimi Sadegh
e-mail: a.rahimisadegh@gmail.com

A. Heidari
School of Electrical Engineering and Telecommunication, University of New South Wales,
Sydney, Australia
e-mail: alireza.heidari@unsw.edu.au

Fr	Number of feeders
$DERM$	Number of DERs
MWI	Maintenance time window
$NDASC$	Number of DA market scenarios
λ	Probability of scenario
ρ^{DA}	Energy price purchased from DA market
NH	Number of DA market hours
E^{DA}	Energy purchased from upward network in DA market
ρ'^{DA}	Energy price sold to DA market
E'^{DA}	Energy purchased to upward network in DA market
NDG	Number of DGs
φ^{DG}	Decision variable for DG commitment
C^{DG}	Operational cost of DG
$NESS$	Number of ESSs
φ^{ESS}	Decision variable for ESS commitment
C^{ESS}	Operational cost of ESS
NIL	Number of ILs
φ^{IL}	Decision variable for IL commitment
C^{IL}	Operational cost of IL
$NCHP$	Number of CHPs
φ^{CHP}	Decision variable for CHP commitment
C^{CHP}	Operational cost of CHP
$NCONT$	Number of contingencies
$ENSC$	Energy not supplied costs
P	Active power generation
Q	Reactive power generation
S_{\max}	Maximum apparent power generation
RU	Ramp up power generation
RD	Ramp down power generation
P^{IL}	Active power interrupted in IL
$\cos\varphi^{IL}$	Power factor of IL
P^{ESS}	Active power of ESS

Sets

I	Index of substation set
J	Index of under maintenance substation set
K	Index of feeder set
l	Index of under maintenance feeder set
m	Index of DER set
n	Index of under maintenance DER set
i'	Index of DA scenarios set
j'	Index of hour-ahead scenarios set

- k' Index of DG set
- l'' Index of ESS set
- m' Index of IL set
- n' Index of CHP set
- l' Index of contingencies set

20.1 Introduction

Distributed Energy Resources (DERs) are widely integrated into power system operational planning paradigms and the DER-based systems are mainly Microgrids (MGs) [1].

As shown in Fig. 20.1, a microgrid can be introduced as a system, which includes DERs such as solar Photo Voltaic (PV) system, Combined Heat and Power (CHP) unit, small Wind Turbine (WT), Electrical Storage System (ESS) and Interruptible Loads (ILs); in a way that it has at least one controllable energy source [1].

The Microgrid Operator (MGO) performs the optimal scheduling of its dispatchable resources by considering the uncertainties of upward electricity market price, intermittent energy resources and ILs [2].

Over recent years, different aspects of optimal scheduling of the microgrid problem have been studied. Ref. [3] presents an optimal stochastic meta-heuristic scheduling algorithm for the networked microgrids considering uncertainties of DERs and Demand Response Programs (DRPs). Reference [4] explores the day-ahead scheduling of CHP systems considering DERs and boilers and considers different scenarios of demand and electricity price.

Reference [5] introduces an optimal day-ahead operational planning algorithm that minimizes pollutant emission and operating cost. The model is solved using a Species-based Quantum Particle Swarm Optimization (SQGA) evolutionary method. Reference [6] proposes a robust optimization algorithm for scheduling of microgrid resources that uses an information gap method to model the wholesale electricity market uncertainties.

Reference [7] presents a bi-level algorithm to optimize interactions between parking lot agent and distribution system operator. The upper-level problem minimizes the cost of DSO; meanwhile, the lower-level problem schedules the parking lot owner resources.

Reference [8] introduces a risk-based optimal scheduling of reconfigurable system that maximizes profit the system operator. The uncertainties of upward network prices, intermittent electricity generation facilities are considered. The optimal combination of system switches is explored using a meta-heuristic optimization method.

Reference [9] introduces a two-stage stochastic algorithm to minimize the reserve cost that is used for compensating the intermittent DER power generation forecast errors.

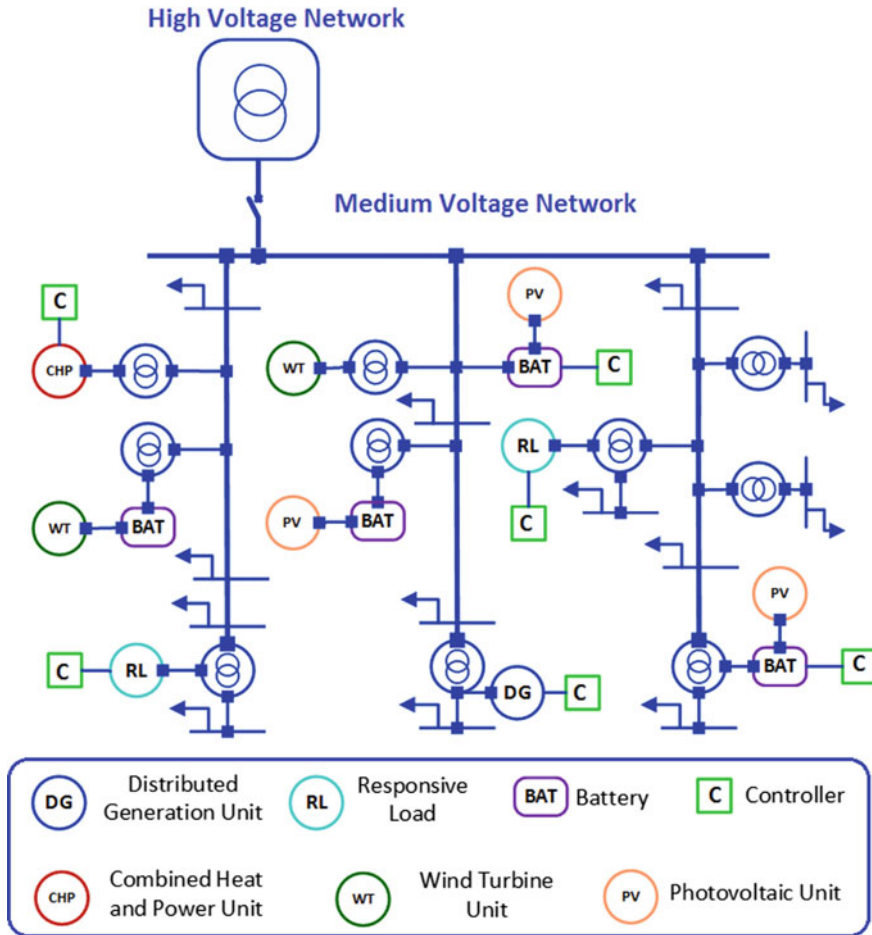


Fig. 20.1 Schematic diagram of a microgrid

Reference [10] presents an algorithm for maximizing of MGO profit considering WT power generation and wholesale market uncertainties. The algorithm uses a stochastic optimization method to model uncertainties.

Reference [11] uses a stochastic optimization algorithm to minimize the operation cost. The uncertainties of the DERs and DRPs are modelled by scenarios and interruptible load bids, respectively. Reference [12] introduces a stochastic scheduling algorithm that the uncertainties of intermittent DERs are modelled by the probability density functions. The results show that the DRP can reduce operating costs. These references do not consider the security constraints and thermal loads.

This book chapter is about the OMOP algorithm that considers the intermittent power generation uncertainties and contingencies scenarios.

20.2 Problem Modelling

The MGO maximizes its profit in the Day-Ahead (DA) market; meanwhile, it minimizes its system’s operational costs. In addition, the DA market price is assumed to depend on unpredictable market conditions, which makes it extremely difficult to investigate the problem by considering the stochastic parameters. Therefore, in this book chapter, the uncertainty of the intermittent energy resource outputs, MG contingencies and the DA market price are modelled with the scenario.

Figure 20.2 shows the MGO interactions with upward network and its DERs.

The MGO must determine the optimal values of problem decision variables. Thus, the OMOP decision variables can be categorized as:

- (1) Maintenance scheduling of MG’s resources,
- (2) Energy generation of MG’s dispatchable energy resources,
- (3) The volume of energy purchased from the upward network.

The system costs can be presented as:

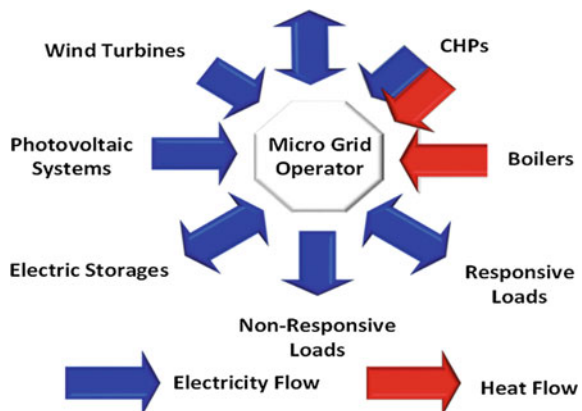
- (1) Operation and maintenance costs of system resources,
- (2) Energy purchased costs,
- (3) The expected profit of energy sold to upward network in the DA market.

The Energy Not Supplied Cost (ENSC) is considered in OMOP as reliability criteria [13].

20.2.1 First Level Problem Formulation

The MGO optimizes its monthly maintenance scheduling and it encounters the uncertainties of power exchanges with the upward network, intermittent power generation,

Fig. 20.2 The MGO interactions



and system contingencies. The first level optimization problem considers the maintenance starting periods, forecasted peak load, and system costs.

The first level problem objective function is proposed as:

$$\begin{aligned}
 \min C_1 = & \sum_{i \in N_{Sub}} \sum_{j \in MW_{Sub}} C_{MC_Sub\ ij} \times (1 - X_{Sub\ ij}) + X_{Sub\ ij} \times C_{OP_Sub\ ij} \\
 & + \sum_{k \in Fr} \sum_{l \in MW_{Fr}} C_{MC_Feed\ kl} \times (1 - X_{Feed\ kl}) + X_{Feed\ kl} \times C_{OP_Feed\ kl} \\
 & + \sum_{m \in DER} \sum_{n \in MW_{DER}} C_{MC_DER\ mn} \times (1 - X_{DER\ mn}) + X_{DER\ mn} \\
 & \times C_{OP_DER\ mn}
 \end{aligned} \tag{20.1}$$

The objective function is decomposed into transformers, feeders and DERs maintenance costs. The first level optimization problem is subjected to maintenance constraints and load flow constraint.

The second level problem deals with optimal MGO estimated costs in DA market for the different scenarios.

20.2.2 Second Level Problem Formulation

At the second level optimization problem, the MGO maximizes its expected profit; meanwhile, it minimizes the system operation costs. The MGO determines the optimal schedule of dispatchable DERs and the energy transacted in the DA market.

$$\begin{aligned}
 \min \sum_{i'=1}^{NDASC} \lambda_i & \left(\sum_{j'=1}^{NH} \rho_{i'j'}^{DA} * E_{i'j'}^{DA} - \sum_{j'=1}^{NH} \rho_{i'j'}^{DA} * E_{i'j'}^{DA} \right. \\
 & + \sum_{k'=1}^{NDG} \varphi_{i'k'}^{DG} \times C_{i'k'}^{DG} + \sum_{k''=1}^{NESS} \varphi_{i'k''}^{ESS} \times C_{i'k''}^{ESS} \\
 & \left. + \sum_{m'=1}^{NIL} \varphi_{i'm'}^{IL} \times C_{i'm'}^{IL} + \sum_{n'=1}^{NCHP} \varphi_{i'n'}^{CHP} \times C_{i'n'}^{CHP} + \sum_{l'=1}^{NCONT} ENSC_{i'l'} \right)
 \end{aligned} \tag{20.2}$$

The objective function consists of the following groups: (1) the costs of energy purchased from the upward wholesale market; (2) the profits of energy sold to the upward network; (3) the commitment of DGs; (4) the commitment of ESSs; (5) the commitment of ILs; (6) the commitment of CHPs; (7) ENSCs.

The objective function is restricted to these constraints:

The maximum and minimum power generations of microgrid energy resources, ramp constraints, minimum up-time and down-time, AC power flow, state of charge and the limits of ESSs that can be written as:

$$P_{Min}^{DG} \cdot \varphi^{DG} \leq P^{DG} \leq P_{Max}^{DG} \cdot \varphi^{DG} \quad (20.3)$$

$$Q_{Min}^{DG} \cdot \varphi^{DG} \leq Q^{DG} \leq Q_{Max}^{DG} \cdot \varphi^{DG} \quad (20.4)$$

$$P_{Min}^{CHP} \cdot \varphi^{CHP} \leq P^{CHP} \leq P_{Max}^{CHP} \cdot \varphi^{CHP} \quad (20.5)$$

$$Q_{Min}^{CHP} \cdot \varphi^{CHP} \leq Q^{CHP} \leq Q_{Max}^{CHP} \cdot \varphi^{CHP} \quad (20.6)$$

$$\sqrt{(Q^{DG})^2 + (P^{DG})^2} \leq S_{Max}^{DG} \quad (20.7)$$

$$(P_{(t+1)}^{DG}) - (P_{(t)}^{DG}) \geq RU^{DG} \quad (20.8)$$

$$(P_{(t)}^{DG}) - (P_{(t+1)}^{DG}) \geq RD^{DG} \quad (20.9)$$

$$\sqrt{(Q^{CHP})^2 + (P^{CHP})^2} \leq S_{Max}^{CHP} \quad (20.10)$$

$$(P_{(t+1)}^{CHP}) - (P_{(t)}^{CHP}) \geq RU^{CHP} \quad (20.11)$$

$$(P_{(t)}^{CHP}) - (P_{(t+1)}^{CHP}) \geq RD^{CHP} \quad (20.12)$$

$$P_{Min}^{IL} \times \varphi^{IL} \leq P^{IL} \leq P_{Max}^{IL} \times \varphi^{IL} \quad (20.13)$$

$$Q^{IL} = (P^{IL}) \sqrt{\frac{1}{\cos \varphi^{IL}} - 1} \quad (20.14)$$

$$\sum_{k=1}^t P_k^{ESS} \leq P_{max}^{ESS} \quad (20.15)$$

20.3 Solution Algorithm

For the first level optimization problem, the Genetic Algorithm (GA) ALGORITHM is used. Figure 20.3 depicts the flowchart of the introduced algorithm. The upper-level problem implements the GA for finding the best solutions of the estimated scenarios; meanwhile, the second level problem uses a mixed-integer nonlinear optimization procedure [13, 14].

The MATLAB software is used to generate random numbers. Then, by connecting the MATLAB to GAMS, the generated scenarios are inserted into GAMS, and scenario reduction is implemented by a forward method. Next, for each of the scenarios, the introduced decomposition method is applied. The scenario generation and reduction procedure are shown in Fig. 20.4.

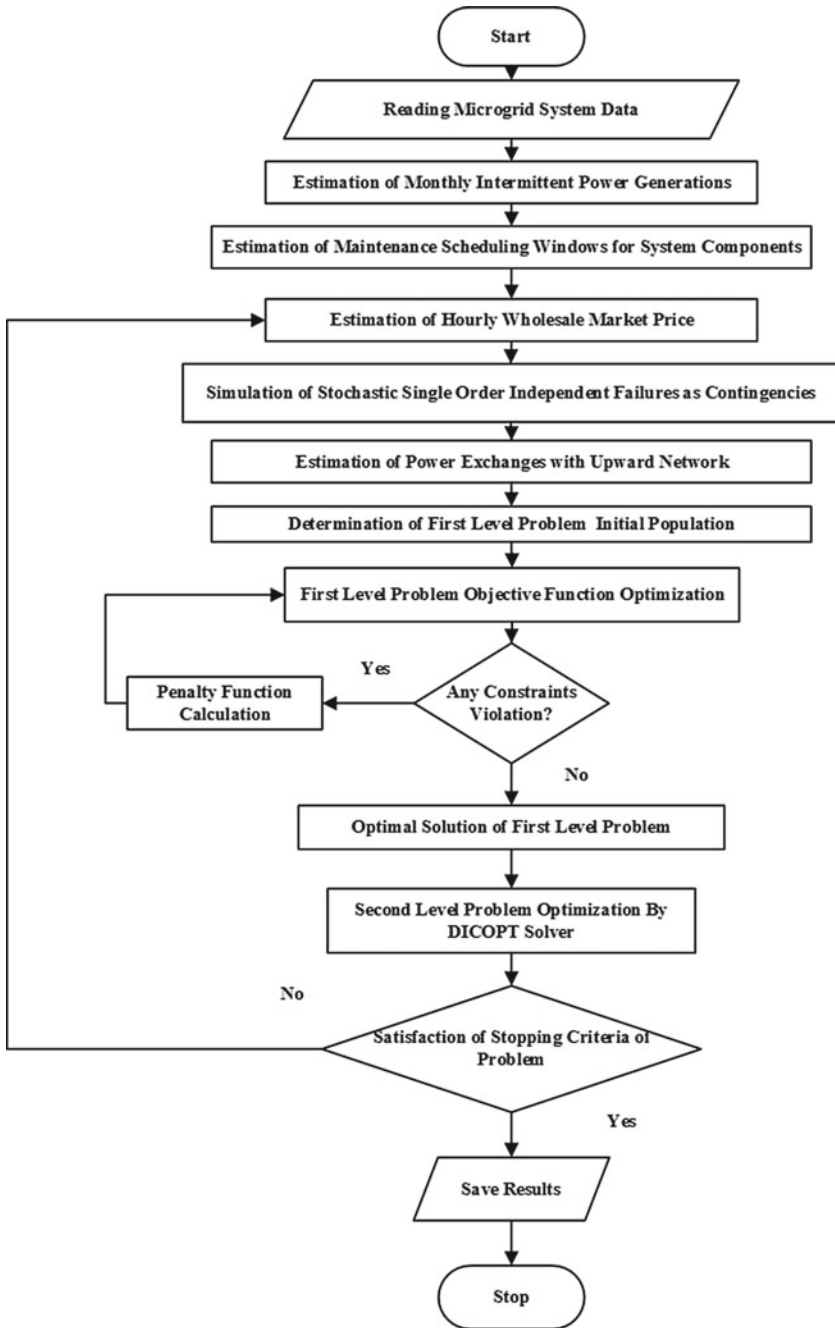


Fig. 20.3 The flowchart of the two-level optimization introduced algorithm

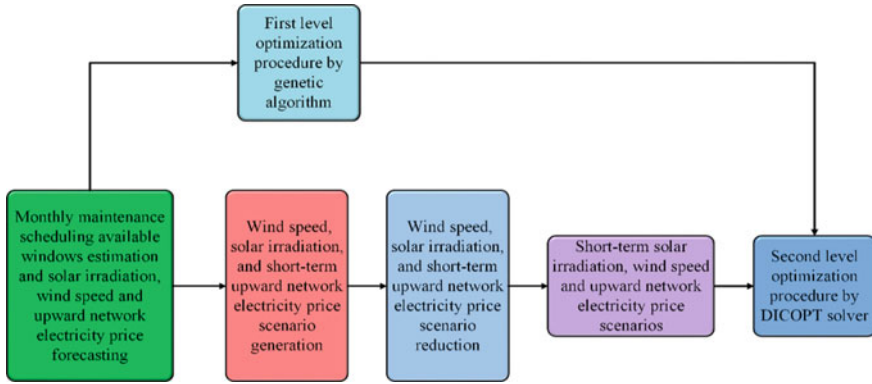


Fig. 20.4 The scenario generation and reduction procedure

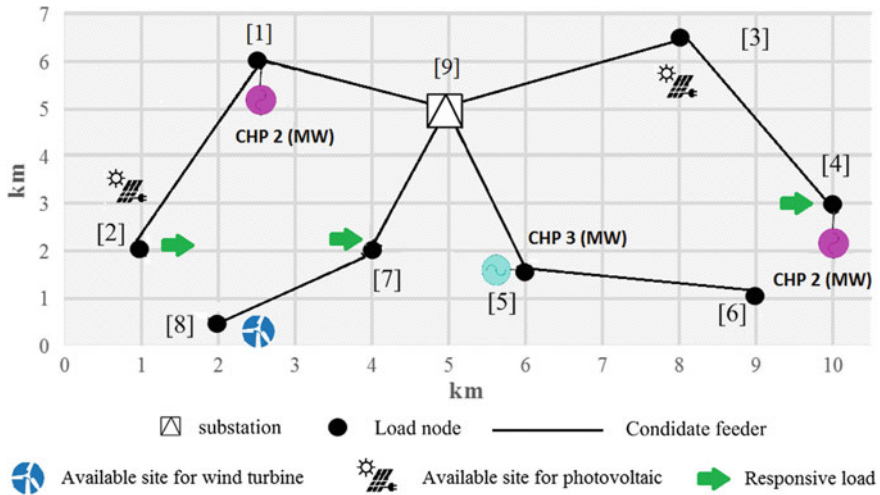


Fig. 20.5 The 9-bus microgrid

20.4 Numerical Results

The introduced model is implemented on the 9-bus and 33-bus test systems. Figures 20.5 and 20.6 depict the 9-bus and 33-bus system, respectively. The 9-bus and 33-bus test system data are presented at [15–18], respectively. The wind turbine and solar panel data are available at [18].

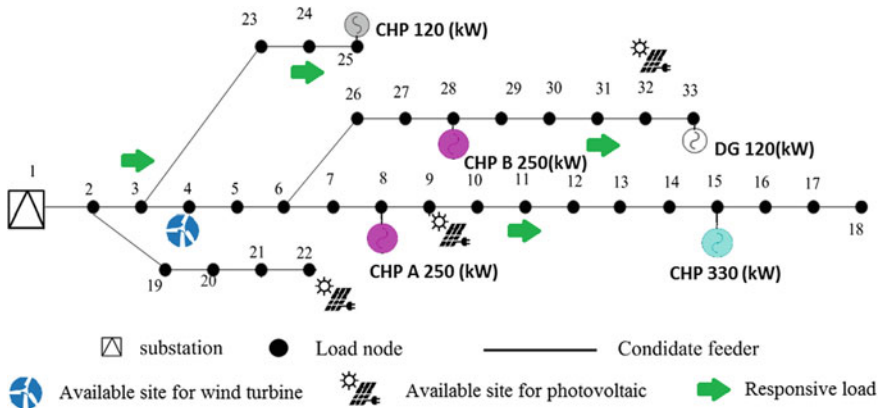


Fig. 20.6 The 33-bus microgrid

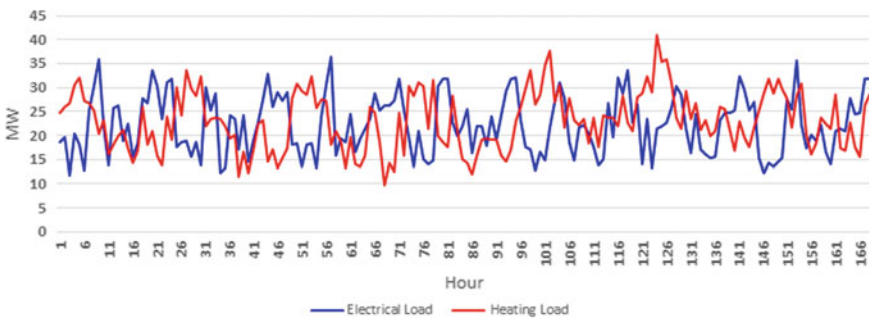


Fig. 20.7 The base load of the 9-bus system

20.4.1 The 9-Bus Test System

Figures 20.7 and 20.8 depict the base load and upward network electricity price of the 9-bus microgrid, respectively.

Table 20.1 presents the optimization input data for the 9-bus system.

Figures 20.9 and 20.10 show the electricity generation of solar photovoltaic panels and wind turbines, respectively.

Figure 20.11 shows the stacked column of the estimated electricity generation of CHPs. As shown in Fig. 20.11, the CHPs are at full load when they are committed. The first CHP is supplying the base electrical load of the MG and the third CHP is supplying the peak electrical load.

Figure 20.12 depicts the heating generation of CHPs and boilers. As shown in Fig. 20.12, the CHPs are at full load when they are committed and the boiler is tracking the heating load.

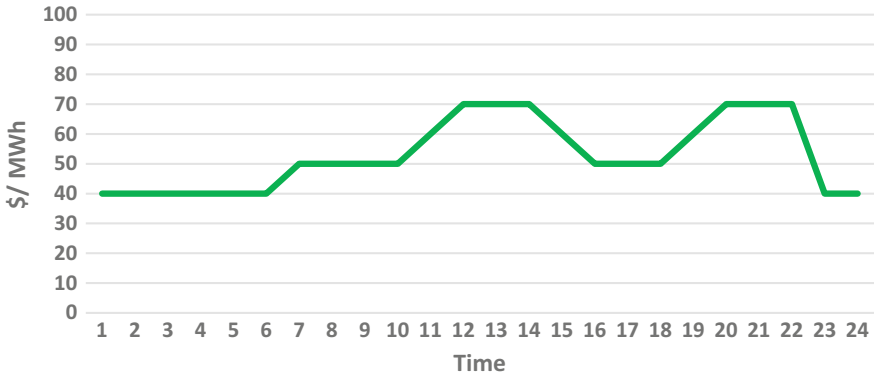


Fig. 20.8 The base electricity price of upward network of the 9-bus system

Table 20.1 The optimization input data for the 9-bus system

Parameter	Value
Discount rate (%)	13
Load power factor	0.90
Load growth rate of (%)	5
Number of solar irradiation scenarios	5000
Number of wind turbine power generation scenarios	6000
Number of upward market price scenarios	500
Number of solar irradiation reduced scenarios	400
Number of wind turbine power generation reduced scenarios	45
Number of upward market price reduced scenarios	15

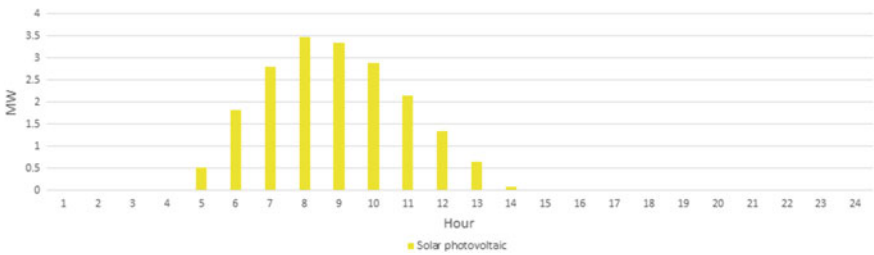


Fig. 20.9 The electricity generation of solar photovoltaic of 9-bus system

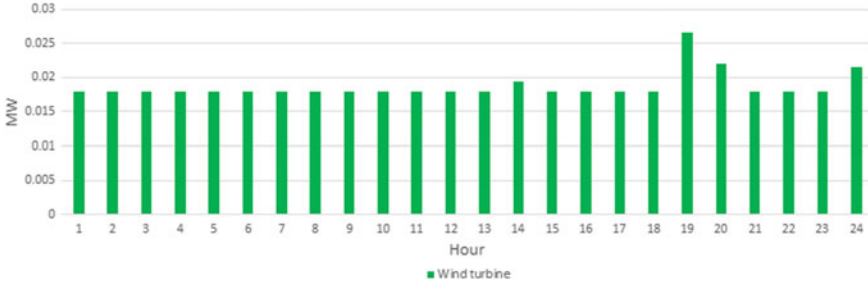


Fig. 20.10 The electricity generation of wind turbines of 9-bus system

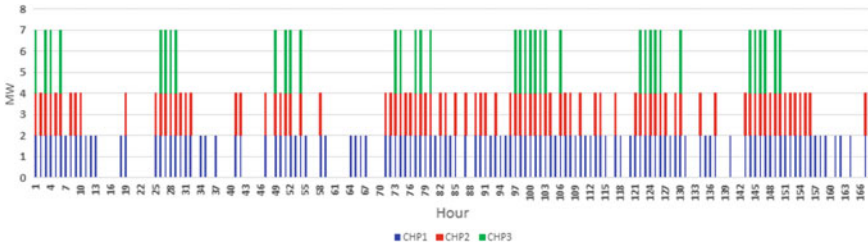


Fig. 20.11 The stacked column of the estimated electricity generation of CHPs of 9-bus system



Fig. 20.12 The stacked column of the estimated heating generation of CHPs and boilers of 9-bus system

Figure 20.13 displays the optimal maintenance scheduling of system for the first half of the year. The optimal maintenance scheduling for the second half of the year is the same as the first one. The OMOP ensures the maintenance workload of the system is evenly distributed across the year. Table 20.2 depicts the optimal operational and maintenance costs of the system.

20.4.2 The 33-Bus Test System

Figure 20.14 depicts the base load of the 33-bus microgrid.

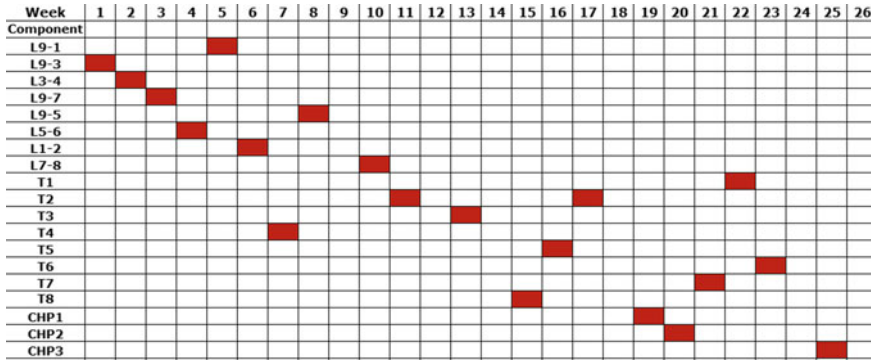


Fig. 20.13 The optimal maintenance scheduling of 9-bus system for the first half of the year

Table 20.2 The optimal aggregated operational and maintenance costs of the 9-bus system

Costs (MMUs)			
CHP operation and maintenance costs (MMUs)	3.9812	Transformers operation and maintenance costs (MMUs)	0.5871
ENSCs	0.36541	IL costs (MMUs)	0.7982
Energy loss costs (MMUs)	0.13815	Energy purchased from upward network costs (MMUs)	0.1974

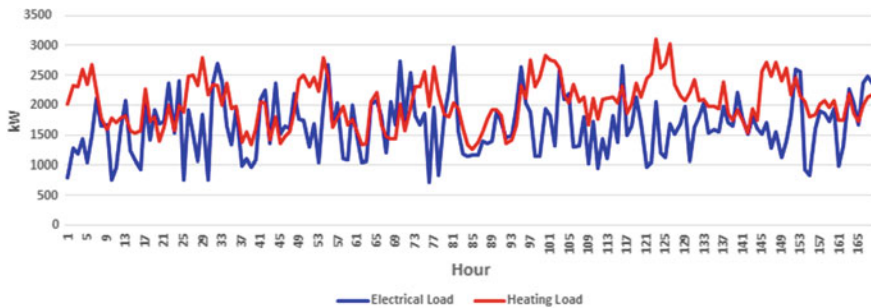


Fig. 20.14 The base load of the 33-bus test system

Figure 20.15 shows the electricity generation of solar photovoltaic panels and wind turbines.

Figure 20.16 presents the stacked column of the estimated electricity generation of CHPs and DGs. As shown in Fig. 20.16, the CHPs and DGs are at full load when they are committed. The CHP250A and CHP330 are fully committed to supplying the base electrical load of the system.

Figure 20.17 depicts the stacked column of the estimated heating generation of CHPs and boilers of the system. The boiler is tracking the heating load.

Figure 20.18 displays the optimal maintenance scheduling for the first half of the year. The optimal maintenance scheduling for the second half of the year is the same

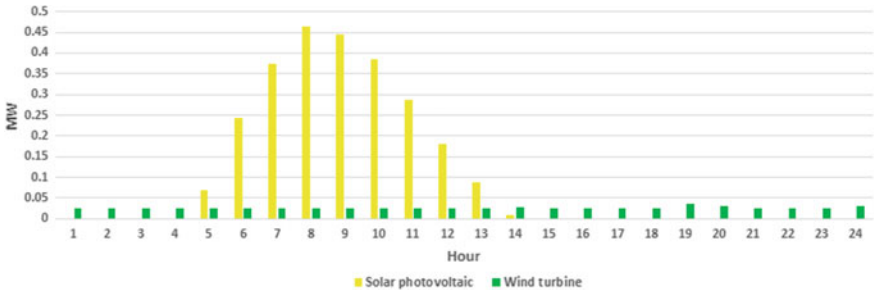


Fig. 20.15 The electricity generation of solar photovoltaic panels and wind turbines of 33-bus system

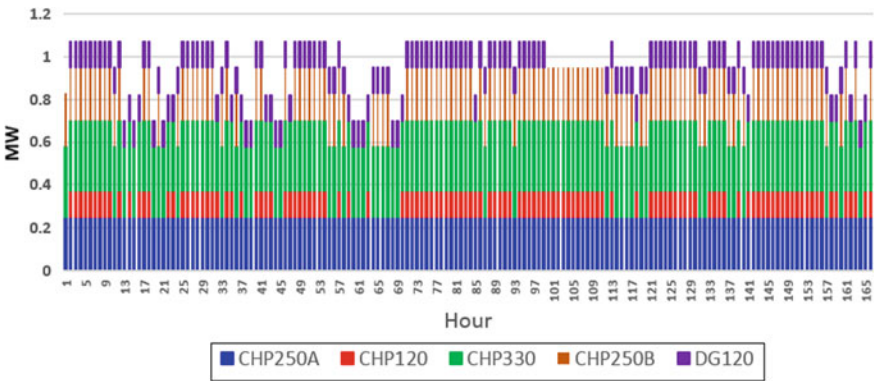


Fig. 20.16 Stacked column of estimated electricity generation of CHPs and DGs of 33-bus system

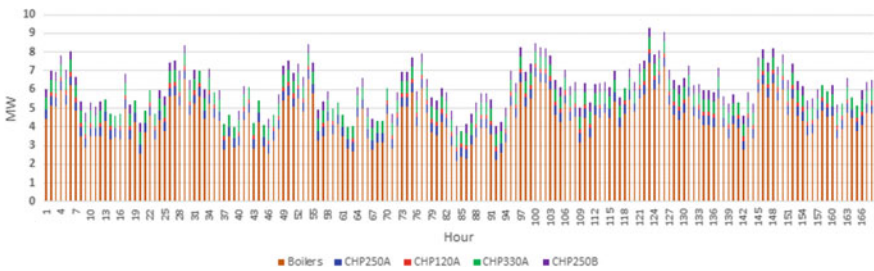


Fig. 20.17 Stacked column of estimated heating generation of CHPs and boilers of 33-bus system

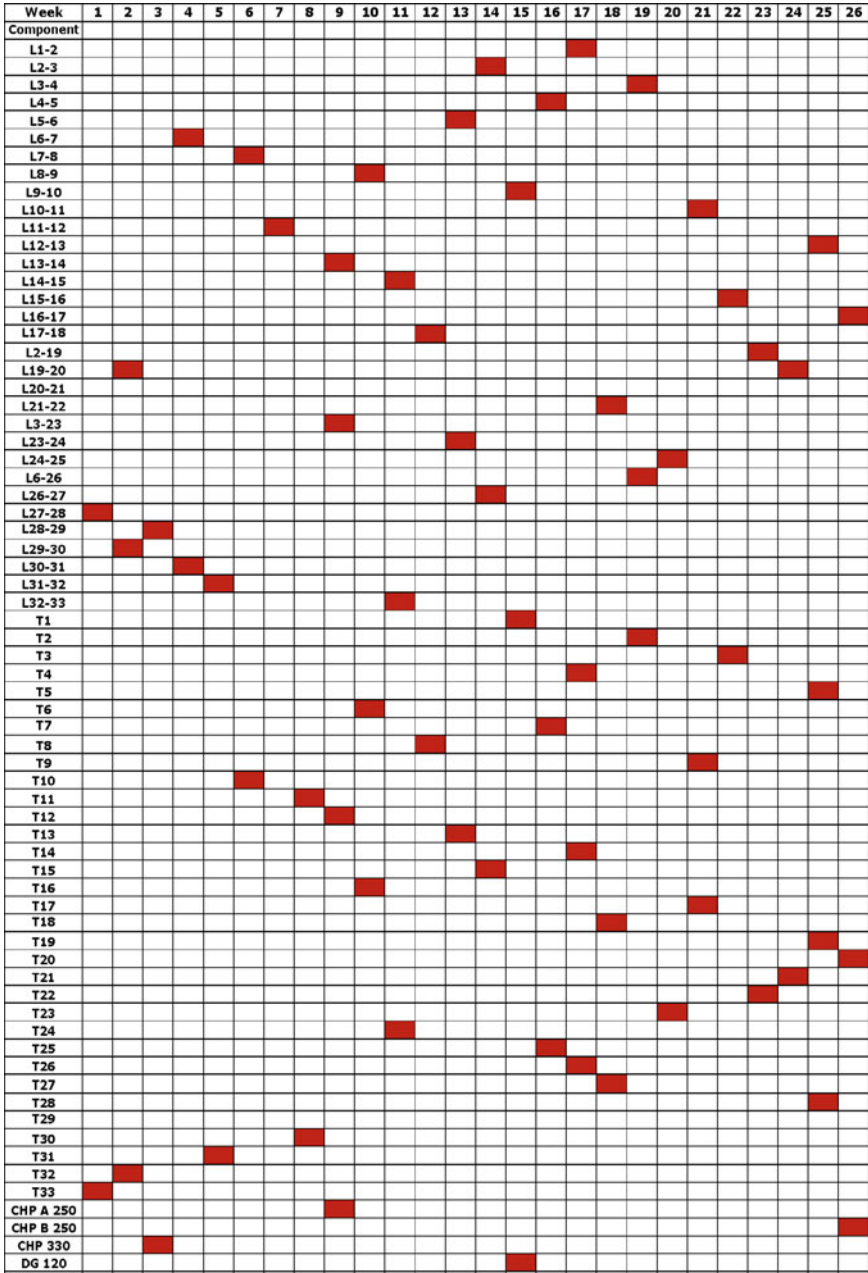


Fig. 20.18 The optimal maintenance scheduling of 33-bus system for the first half of the year

Table 20.3 The optimal aggregated operational and maintenance costs of the 33-bus system

Costs (MMUs)			
CHP and DG operation and maintenance costs (MMUs)	12.3918	Transformers operation and maintenance costs (MMUs)	2.6918
ENSCs	0.3487	IL costs (MMUs)	4.1287
Energy loss costs (MMUs)	0.3915	Energy purchased from upward network costs (MMUs)	0.3621

as the first one. The optimization algorithm distributes the maintenance workload across the year.

Table 20.3 depicts the optimal operational and maintenance costs of the 33-bus system for the operational planning horizon.

20.5 Conclusions

A microgrid optimal operational planning framework was reviewed in the present chapter. The introduced method used a two-level optimization model to investigate the intermittent power generations and ILs impacts on the OMOP problem. The proposed framework for OMOP considered the system uncertainties and the problem explores the optimal maintenance scheduling and operation. The OMOP procedure had a great non-convex discrete state space and the proposed solution algorithm had the ability to model the nonlinearity and non-convexity of the system's state space and the dynamic coupling constraints of the electric and heating systems.

The model of OMOP was a MINLP problem, and the GA algorithm was used for the first level problem. The second level problem utilized the DICOPT solver. The algorithm was assessed for the 9-bus and the 33-bus test systems with quite acceptable results.

In conclusion, the adoption of the proposed OMOP includes maintenance scheduling allows increasing significantly the microgrid benefits and reliability.

References

1. S. Chowdhury, S.P. Chowdhury, P. Crossley, Microgrids and active distribution networks. IET Renewable Energy Series (2009)
2. N.I. Nwulu, X. Xia, Optimal dispatch for a microgrid incorporating renewables and demand response. *Renew. Energy* **101**, 16–28 (2017)
3. N. Nikmehr, S. Najafi Ravadanegh, A. Khodaei, Probabilistic optimal scheduling of networked microgrids considering time-based demand response programs under uncertainty. *Appl. Energy* **198**, 267–279 (2017)

4. M. Alipour, B. Mohammadi Ivatloo, K. Zare, Stochastic risk-constrained short-term scheduling of industrial cogeneration systems in the presence of demand response programs. *Appl. Energy* **136**, 393–404 (2014)
5. V. Hosseinnezhad, M. Rafiee, M. Ahmadian, P. Siano, Optimal day-ahead operational planning of microgrids. *Energy Convers. Manag.* **126**, 142–157 (2016)
6. J. Aghaei, V.G. Agelidis, M. Charwand, F. Raeisi, A. Ahmadi, A. Esmaeel Nezhad, A. Heidari, Optimal robust unit commitment of CHP plants in electricity markets using information gap decision theory. *IEEE Trans. Smart Grid* **8**, 2296–304 (2017)
7. S. Aghajani, M. Kalantar, Operational scheduling of electric vehicles parking lot integrated with renewable generation based on bilevel programming approach. *Energy* **39**, 422–432 (2017)
8. M. Hemmatia, B. Mohammadi Ivatlooa, S. Ghasemzadeha, E. Reihanib, Risk-based optimal scheduling of reconfigurable smart renewable energy based microgrids. *Int. J. Electr. Power Energy Syst.* **101**, 415–428 (2018)
9. M. Mazidi, A. Zakariazadeh, Sh Jadid, P. Siano, Integrated scheduling of renewable generation and demand response programs in a microgrid. *Energy Convers. Manag.* **86**, 1118–1127 (2014)
10. M. Alipour, B. Mohammadi Ivatloo, K. Zare, Stochastic scheduling of renewable and CHP—based microgrids. *IEEE Trans. Ind. Inform.* **11**, 1049–58 (2015)
11. M.H. Shams, M. Shahabi, M.E. Khodayar, Stochastic day-ahead scheduling of multiple energy carrier microgrids with demand response. *Energy* **155**, 326–338 (2018)
12. A. Zakariazadeh, S. Jadid, P. Siano, Smart microgrid energy and reserve scheduling with demand response using stochastic optimization. *Elect. Power Energy Syst.* **63**, 523–533 (2014)
13. M. Setayesh Nazar, M.R. Haghifam, M. Nazar, A scenario driven multiobjective Primary–Secondary microgrid Expansion Planning algorithm in the presence of wholesale–retail market. *Int. J. Electr. Power Energy Syst.* **40**, 29–45 (2012)
14. F. Shahnia, A. Arefi, G. Ledwich, in *Electric Distribution Network Planning* (Springer, 2018)
15. W. El Khattam, K. Bhattacharya, Y. Hegazy, M.M.A. Salama, Optimal investment planning for distributed generation in a competitive electricity market. *IEEE Trans. Power Syst.* **19**(3), 1674–1684 (2004)
16. W. El Khattam, Y.G. Hegazy, M.M.A. Salama, An integrated distributed generation optimization model for distributed system planning. *IEEE Trans. Power Syst.* **20**(2), 1158–1165 (2005)
17. H. Falaghi, M.R. Haghifam, ACO based algorithm for distributed generation sources allocation and sizing in distribution systems, in *Power Tech, IEEE Transactions on Power Systems* (2007), pp. 555–560
18. S.Y. Derakhshandeh, A.S. Masoum, S. Deilami, M.A.S. Masoum, M.E.H. Golshan, Coordination of generation scheduling with PEVs charging in industrial microgrids. *IEEE Trans. Power Syst.* **28**(3), 3451–3461 (2013)